Temperature-dependent disorder in a natural Mg-Al-Fe^{2+}-Fe^{3+}-spinel

ANTONIO DELLA GIUSTA, SUSANNA CARBONIN

Dipartimento di Mineralogia e Petrologia, Università di Padova, Corso Garibaldi 37, 35122 Padova, Italy

AND

GIULIO OTTONELLO

Dipartimento di Scienze della Terra, Università di Genova, Corso Europa 26, 16132 Genova, Italy

Abstract

A natural Mg-Al-Fe spinel from the Balmuccia peridotite (Italian Western Alps) was annealed at T between 650 and 1150°C, under controlled oxygen activity, and quenched in H_2O. Twenty-three cation distributions were calculated from XRD structural refinements in tandem with microprobe analysis, and verified by Mössbauer spectroscopy in the case of unheated samples.

Unheated crystals showed essentially ordered distribution of Fe^{3+} in octahedral and Fe^{2+} in tetrahedral sites, the only intracrystalline disorder being represented by ~0.12 atoms per formula unit of $^{[4]}Al$ and $^{[6]}Mg$. Thermal runs and quenching maintained substantially ordered distribution of Fe^{2+} and Fe^{3+} up to ~990°C and produced continuous $^{[4]}Mg$-$^{[6]}Al$ exchange. Between 990 and 1150°C, the previous order of Fe^{2+}-Fe^{3+} appeared to change slightly, $^{[6]}Fe^{2+}$ reaching ~0.04 afu and $^{[6]}Mg \cong {}^{[4]}Al \cong 0.24$ afu at the highest T. After quenching from this temperature, Fe^{2+} still resided mainly in the T site. Some previously heated crystals underwent reordering on lowering of the temperature.

Experimental data, integrated with existing literature, enabled cation-oxygen distance in this structure to be improved. Results from annealed samples allowed the formulation of an experimental thermometric function based on Mg-Al intracrystalline disorder.

KEYWORDS: spinel, disorder, temperature dependence, peridotite, Italian Alps.

Introduction

SPINELS are common accessory minerals in many rocks; due to their magnetic properties, they are of great interest in geophysical research and in the ceramics industry. As petrogenetic indicators, they have been investigated by Irvine (1965), Sack (1982), Gasparik and Newton (1984) and Sack and Ghiorso (1991*a*), among others. Site populations have been investigated in synthetic magnetite by Wu and Mason (1981), Trestman-Matts *et al.* (1983); in synthetic $MgAl_2O_4$ by Grimes *et al.* (1982), Yamanaka and Takeuchi (1983), Peterson *et al.* (1991), Millard *et al.* (1992); in synthetic $FeAl_2O_4$ by Larsson *et al.* (1994); in synthetic $MgCr_2O_4$, $ZnCr_2O_4$, Fe_3O_4, $ZnAl_2O_4$ by O'Neill and Dollase (1993); in synthetic $NiAl_2O_4$ by O'Neill *et al.* (1991); in synthetic $ZnFe_2O_4$ by O'Neill (1992); in synthetic $MgFe_2O_4$ by O'Neill *et al.* (1992), and in several binary joins by Nell *et al.* (1989), Waerenborgh *et al.* (1994). Thermodynamic modelling of spinels has also been studied by Petric and Jacob (1982), Urusov (1983), O'Neill and Navrotsky (1983), Ottonello (1986), Sack and Ghiorso (1991*b*), and Della Giusta and Ottonello (1993).

Spinel structure (Hafner, 1960; Hill *et al.*, 1979) has $Fd3m$ symmetry, and with only the oxygen atom with (u, u, u) independent fractional coordinates and a multiplicity of 32. Eight cations lie in a tetrahedral site (T) with $\bar{4}3m$ symmetry, coordinates (1/8, 1/8, 1/8), and sixteen in an octahedral site (M), with coordinates (1/2, 1/2, 1/2). These refer to the origin at centre ($\bar{3}m$). The M site has $\bar{3}m$ symmetry, and may be slightly distorted being elongated or shortened

Mineralogical Magazine, August 1996, Vol. 60, pp. 603–616

along the three-fold axis following the (u, u, u) oxygen coordinates. M is a perfect octahedron for u = 0.25. The oxygen atom is surrounded by three M and one T cations, forming a triangular pyramid with $3m$ symmetry. Thus the structure is defined by only two cation-to-oxygen distances, T–O and M–O, which are related to the a cell parameter and to u by the following equations:

$$a = \frac{8}{11\sqrt{3}}\left[5(\mathrm{T}-\mathrm{O}) + \sqrt{33(\mathrm{M}-\mathrm{O})^2 - 8(\mathrm{T}-\mathrm{O})^2}\right] \quad (1)$$

$$u = \frac{0.75\mathrm{R} - 2 + \sqrt{\frac{33}{16}\mathrm{R} - 0.5}}{6(\mathrm{R}-1)} \quad (2)$$

where $\mathrm{R} = (\mathrm{M\text{-}O})^2/(\mathrm{T\text{-}O})^2$.

In previous papers (Basso *et al.*, 1984; Della Giusta *et al.*, 1986, 1987; Princivalle *et al.*, 1989), we investigated several natural samples from various geological environments. One result was that a depends mainly on bulk chemistry, while u, being determined by cation distribution, is strongly affected by physical environment. One of the previously investigated spinels (TS2) has now been selected to measure changes in site population due to temperature. Rock sample TS2 comes from a suite of websteritic dykes crossing a peridotite of mainly lherzolitic composition in the Ivrea-Verbano area, Italian Western Alps (Pizzolon, 1991). This suite, named 'Al-augite suite' (Comin-Chiaramonti *et al.*, 1982), contains spinel with low Cr content, the Cr/(Cr + Al) ratio generally being < 0.04. Very slow cooling during uplift allowed strong exsolution phenomena to take place in the associated pyroxene, so that highly ordered Mg-Al distribution is to be expected in TS2 spinels (Princivalle *et al.*, 1989; Schmocker and Waldner, 1976; Cynn *et al.*, 1993; Peterson *et al.*, 1991; Yamanaka and Takeuchi, 1983). In these spinels, as in spinel *sensu stricto*, completely ordered distribution means all divalent cations in the T site and all trivalent ones in the M site.

Experimental

Firstly, the homogeneity of TS2 spinels was tested by microprobe in 103 randomly chosen points of one thin section. Single grains showed sufficiently good enough homogeneity, while chemical composition was quite different from grain to grain, above all as far as Cr content was concerned (average wt.% Cr_2O_3 = 2.48, σ = 1.12).

Several crystals extracted from the same rock hand-specimen had to be examined to find some suitable for single-crystal data collection. Seven of these, named A–G, were found for the experiments reported below. They shared both similar cell parameters and Cr content – the latter being much lower than the average on the hundred analysed points. This similarity provided some guarantee of the possibility of carrying out experiments on seven crystals as if they were just one.

Three of the crystals had already been the subject of a comparison between Mössbauer spectroscopy and X-ray refinement results (Carbonin *et al.*, 1996). The homogeneity, both intra- and intercrystalline, of TS2 spinels was more extensively reported in that work.

Single-crystal X-ray diffraction

Unit cell parameters were obtained on a single-crystal STOE AED4 diffractometer with Mo-$K\alpha$ radiation, monochromatized by a graphite crystal: 22 reflections in the range $8° < \theta < 20°$ were accurately centred; a stepscan through each reflection was made at positive 2θ and ω and the centre of gravity was calculated. Then reflections were scanned at negative 2θ and ω and the centres were again determined. The mean of the ω centres was taken as the true θ value. The diffractometer alignment was checked by measuring the cell parameters of a quartz crystal and a ruby supplied by the Organizing Committee of the XII Congress of the IUC. Diffraction data were collected up to $2\theta = 100°$. The ω–2θ scan mode was used with peak-base widths of $2\theta = 2°$, 45-step integration, 0.6 s per step counting time. The data collection of crystal TS2A1 was performed for a P lattice. A few reflections forbidden in the spinel space group $Fd3m$ were detected, but a ψ scan showed that they were due to multiple reflections. Thus, all the other data were collected for an F lattice. Up to six equivalent reflections were measured and corrected for absorption and background, following North *et al.* (1968) and Blessing *et al.* (1972) respectively. After correction for Lorentz and polarization effects and isotropic secondary extinction, a set of ~170 observed structure factors Fo_{hkl} was obtained from each crystal (Table 1).

Crystal structure refinement

Structural refinements were performed in the $Fd3m$ space group. Two neutral scattering curves, Mg *vs* Fe in the T site and Al *vs* Fe in the M site, were assigned in the initial stage of the refinement, with the constraints of full site occupancy and equal displacement parameters. No constraint from chemical analyses was imposed.

Calculations executed against Fo_{hkl} turned out to be rather unstable and dependent on the σ threshold used. Consequently, structural refinements were

TABLE 1. Crystal data in natural unheated and heated spinels

Sample	T (°C)	t	a (Å)	u	$N_{4\sigma}$	$R_{4\sigma}$	R_{all}	$Ext.'$	U'(T) (Å^2)	U'(M) (Å^2)	U'(Ox) (Å^2)	T-O (Å)	M-O (Å)	e(T)	e(M)	e_{total}
TS2A1	unheat.		8.1104 (4)	0.26362 (7)	172	0.030	0.032	9.16	86 (2)	74 (2)	87 (2)	1.9473 (10)	1.9235 (5)	15.26 (12)	13.38 (6)	42.03
TS2A2	630	2 h	8.1099 (3)	0.26361 (8)	171	0.037	0.038	12.53	91 (3)	78 (2)	91 (2)	1.9470 (11)	1.9234 (6)	15.38 (15)	13.43 (7)	42.23
TS2A3	830	90 m	8.1106 (4)	0.26258 (8)	170	0.030	0.032	11.28	91 (2)	79 (2)	110 (2)	1.9327 (11)	1.9310 (6)	15.48 (12)	13.38 (6)	42.23
TS2A4	990	10 m	8.1100 (3)	0.26225 (8)	170	0.031	0.032	11.07	91 (2)	77 (2)	115 (2)	1.9279 (11)	1.9333 (6)	15.63 (13)	13.39 (6)	42.41
TS2A5	990	70 m	8.1100 (3)	0.26198 (10)	167	0.037	0.038	11.84	95 (3)	82 (2)	122 (2)	1.9241 (14)	1.9352 (7)	15.60 (15)	13.46 (7)	42.52
TS2A6*	920	2 h	8.1096 (4)	0.26194 (13)	172	0.044	0.045	2.93	67 (3)	57 (3)	96 (3)	1.9235 (18)	1.9354 (10)	15.34 (17)	13.37 (9)	42.08
TS2B1	unheat.		8.1108 (4)	0.26361 (7)	165	0.031	0.034	8.77	86 (2)	72 (2)	87 (2)	1.9472 (10)	1.9237 (5)	15.28 (13)	13.40 (6)	42.08
TS2B2	695	110 m	8.1113 (3)	0.26359 (7)	170	0.030	0.032	9.49	81 (2)	66 (2)	81 (2)	1.9471 (10)	1.9239 (5)	15.38 (12)	13.33 (6)	42.04
TS2B3	915	60 m	8.1089 (4)	0.26215 (9)	168	0.033	0.035	10.35	90 (2)	77 (2)	115 (2)	1.9263 (13)	1.9337 (7)	15.40 (13)	13.41 (6)	42.22
TS2B4*	820	2 h	8.1094 (3)	0.26244 (9)	154	0.030	0.034	10.00	88 (2)	75 (2)	109 (2)	1.9305 (13)	1.9317 (7)	15.55 (14)	13.36 (6)	42.27
TS2B5*	730	70 h	8.1097 (3)	0.26261 (7)	166	0.027	0.035	9.33	91 (2)	78 (2)	109 (2)	1.9329 (10)	1.9306 (5)	15.47 (11)	13.33 (6)	42.13
TS2C1	unheat.		8.1113 (4)	0.26354 (8)	174	0.033	0.035	7.67	86 (2)	71 (2)	85 (2)	1.9464 (11)	1.9243 (6)	15.33 (14)	13.41 (7)	42.15
TS2C2	730	46 h	8.1105 (3)	0.26307 (8)	169	0.031	0.034	8.46	89 (2)	74 (2)	99 (2)	1.9396 (11)	1.9275 (6)	15.60 (13)	13.39 (6)	42.37
TS2C3*	695	170 h	8.1097 (4)	0.26298 (9)	171	0.040	0.042	11.56	89 (3)	76 (2)	100 (2)	1.9381 (13)	1.9279 (7)	15.55 (16)	13.46 (7)	42.47
TS2C4*	695	340 h	8.1111 (3)	0.26303 (9)	168	0.037	0.039	9.39	90 (3)	76 (2)	102 (2)	1.9392 (13)	1.9279 (7)	15.50 (14)	13.39 (6)	42.27
TS2D1	unheat.		8.1143 (3)	0.26361 (7)	171	0.031	0.033	9.02	86 (2)	71 (2)	85 (2)	1.9481 (10)	1.9245 (5)	15.44 (13)	13.51 (6)	42.46
TS2D2	650	31 d	8.1138 (3)	0.26349 (7)	168	0.029	0.033	7.92	89 (2)	75 (2)	90 (2)	1.9463 (10)	1.9252 (5)	15.60 (11)	13.47 (5)	42.55
TS2D3	675	24 d	8.1151 (3)	0.26348 (7)	167	0.027	0.031	8.56	84 (2)	71 (2)	88 (2)	1.9464 (10)	1.9256 (5)	15.61 (11)	13.47 (5)	42.54
TS2E1	unheat.		8.1081 (5)	0.26363 (5)	168	0.020	0.023	4.03	76 (2)	62 (1)	75 (1)	1.9469 (7)	1.9229 (4)	15.31 (10)	13.35 (4)	42.02
TS2F1	unheat.		8.1122 (4)	0.26359 (6)	173	0.029	0.030	11.88	88 (2)	76 (2)	92 (2)	1.9473 (8)	1.9241 (4)	15.27 (12)	13.43 (6)	42.13
TS2G1	unheat.		8.1136 (3)	0.26367 (6)	167	0.025	0.032	5.93	87 (2)	71 (2)	85 (2)	1.9488 (8)	1.9239 (4)	15.40 (11)	13.38 (5)	42.16
TS2G2	1150	3 m	8.1121 (4)	0.26176 (8)	166	0.028	0.033	4.81	90 (2)	77 (2)	121 (2)	1.9216 (11)	1.9373 (6)	15.56 (11)	13.50 (6)	42.55
TS2G3	1150	100 m	8.1107 (4)	0.26168 (8)	168	0.031	0.035	8.26	88 (2)	77 (2)	122 (2)	1.9201 (11)	1.9376 (6)	15.48 (12)	13.45 (6)	42.39
TS2B6§	680	120 d	8.0875 (9)	0.26091 (7)	155	0.019	0.021	2.26	67 (2)	67 (1)	107 (2)	1.9038 (10)	1.9377 (6)	14.50 (10)	13.24 (6)	40.98
TS2C5§	680	120 d	8.0891 (6)	0.26107 (8)	153	0.026	0.029	3.02	78 (2)	75 (2)	113 (2)	1.9064 (11)	1.9369 (6)	14.61 (11)	13.28 (6)	41.17
TS2D4§	680	120 d	8.0850 (9)	0.26073 (7)	157	0.024	0.025	2.56	78 (2)	78 (2)	119 (2)	1.9007 (10)	1.9384 (6)	14.29 (11)	13.22 (6)	40.74

Notes: In sample list, last character (number) refers to different experiments on same crystal; the last but one (letter) refers to different crystals from TS2 sample. Residual index R calculated using Fo_{hkl}.

* Ordering runs; § oxidized samples; $N_{4\sigma}$: reflections > 4σ; $R_{4\sigma}$: residual index for reflections > 4σ; R_{all}: residual index for all reflections; $Ext.' = Ext \cdot 10^3$; $U' = U_{eq} \cdot 10^4$.

performed against Fo^2_{hkl} using the SHELX-93 program (Sheldrick, 1993). Recovering all information from the relatively large number of weak reflections with $I > 2\sigma(I)$, stable refinements were obtained and all correlations involving site occupancies disappeared, allowing simultaneous minimization of all structural parameters. The refined parameters were: scale factor, secondary extinction coefficient (*Ext.*), oxygen coordinate (u), tetrahedral and octahedral site occupancies, occ.(T) and occ.(M), and displacement parameters, U(Ox), U(T) and U(M).

Site occupancies depended only slightly on the ionization level of the oxygen scattering curve, while the cation ionization level was irrelevant. Refinements of all crystals were repeated systematically, changing the scattering curves to obtain the best values of all conventional agreement factors over all $\sin\theta/\lambda$ intervals. The best results were obtained with neutral cations and $O^{-1.4}$.

Table 1 shows the crystallographic data obtained. Residual R factors were calculated using Fo_{hkl} instead of Fo^2_{hkl}, for comparison with conventional refinements.

Microprobe analysis on X-ray refined crystals

After X-ray data collection, chemical analysis was performed on the polished surface of the same single crystal used for the XRD study. Composition was obtained by the Cameca/Camebax electron microprobe at the Dept. of Mineralogy and Petrology of the University of Padova. Analyses were performed at 15 kV and 15 nA sample current, using only the WDS method. X-ray counts were converted into oxide weight percentages using a PAP correction program provided by Cameca. Synthetic oxide standards were used, and results were monitored against the same standards. Analyses were carried out after a check that I_{Xstd}/I_{std} was 1.00 ± 0.01 for each element, where I_{Xstd} was the intensity of the analysed standard and I_{std} the intensity of the same standard monitored after each element calibration. Typically, analyses for MgO, FeO and Al_2O_3 were accurate to within 1% of the amounts present, and for minor elements MnO, ZnO, TiO_2, Cr_2O_3, NiO and SiO_2 to within 5%. At least five point analyses were performed on each crystal. The Fe^{3+} was calculated on the basis of three cations per four oxygens; its σ was obviously much higher than the others, since it was affected by those of all the remaining cations.

Table 2 reports the chemical data of the investigated crystals before thermal runs. The total number of electrons obtained from chemical analyses agrees with that from site occupancies, the differences always being $< 0.3e^-$. The TS2C crystal was not analysed before thermal runs and was assigned the same composition as crystal B, on the basis of a similarity.

Thermal runs

Heating experiments were then undertaken in order to study structure and site population variations at various T. Some crystals were heated at first increasing (disordering) and then decreasing temperatures (ordering), with the aim of ascertaining if, at a given temperature, they showed the same structure and site population on both heating and cooling.

The crystals were sealed in SiO_2 tubes, 2 mm ∅, containing iron-wustite buffer wrapped in platinum foil, to prevent reaction between iron and silica. The tubes were filled with argon purified on molecular sieves and titanium sponges. Heating experiments were performed in a vertical furnace with temperature control accurate to ± 5°C; quench was obtained by dropping the sealed tubes into cold water. For an estimate of cooling rate, an insulated thermocouple was inserted in a SiO_2 tube and connected to a high-speed recorder. The tube was flame-heated to 1100°C and then dropped into cold water from the same height as the sealed tubes. This sequence was repeated several times and indicated a time of ~ 0.5 s for a T decrease from 1100 to 400°C. The temperature and duration of each run are reported in Table 1. Five crystals were used for eleven disordering and five reordering thermal experiments. After each run, the crystals were remounted in the same position on the diffractometer, to minimize the differences in absorption correction of the new data collection. Microprobe analyses repeated at the end of thermal runs showed no appreciable variations, in spite of strong reducing conditions. However, some runs produced oxidized samples. The SiO_2 tubes allowed experiments up to 1150°C for ~ 10 hours and up to 700°C for 30 days. Longer durations caused incipient recrystallization of the tube and the entrance of air through silica grain boundaries, with consequent oxidation even of spinel iron. In some samples, oxidation produced very thin lamellae of haematite, identified by its morphology, reflectance, colour and anisotropy. The crystal data for these samples, which will be the subject of future studies, are reported in Table 1 (bottom three rows) for comparison purposes only.

Crystallographic results

Crystal data are reported in Table 1. In the unheated crystals, a ranges from 8.1081 (TS2E1) to 8.1143 Å (TS2D1), an interval about fifteen times wider than the mean σ of the a determinations. The higher a values correspond to higher contents of larger

TABLE 2. Microprobe analysis on X-Ray refined crystals, on basis of 3 cations and 4 oxygens

	TS2A	TS2B-C	TS2D	TS2E	TS2F	TS2G
Al_2O_3	65.33	65.30	64.44	65.01	64.61	64.45
FeO	13.43	12.34	13.83	13.13	13.62	13.78
MgO	20.58	20.69	19.94	20.49	20.16	19.94
MnO	0.11	0.10	0.09	0.09	0.10	0.09
SiO_2	n.a.	0.05	n.a.	0.03	0.03	n.a.
ZnO	0.11	0.13	0.11	0.00	0.10	0.11
Cr_2O_3	0.33	0.64	0.95	0.16	0.50	0.90
NiO	n.a.	0.33	0.29	0.25	0.39	0.34
TiO_2	0.04	0.03	0.05	0.03	0.05	0.11
Total	99.93	99.60	99.71	99.58	99.56	99.72
Al	1.935	1.938	1.924	1.938	1.927	1.924
Fe^{2+}	0.225	0.214	0.238	0.221	0.229	0.238
Fe^{3+}	0.057	0.046	0.055	0.057	0.059	0.054
Mg	0.771	0.777	0.753	0.773	0.761	0.753
Mn	0.002	0.002	0.002	0.002	0.002	0.002
Si	n.a.	0.001	n.a.	0.001	0.001	n.a.
Zn	0.002	0.002	0.002	0.000	0.002	0.002
Cr	0.006	0.013	0.019	0.003	0.010	0.018
Ni	n.a.	0.007	0.006	0.005	0.008	0.007
Ti	0.001	0.000	0.001	0.001	0.001	0.002
Total	3.000	3.000	3.000	3.000	3.000	3.000
$e_{chem.}$*	42.04	41.91	42.42	42.01	42.28	42.42

* Total number of electrons calculated from microprobe analysis: compare with Table 1, last column.
n.a. = not analysed.

cations, Fe^{2+} and Cr, whose sum ranges from 0.224 (TS2E1) to 0.257 afu (TS2D1) (see Table 2). These compositional differences do not affect the oxygen coordinate u, whose range is only 0.00013, less than twice the mean σ. Site occupancies and derived number of electrons in the T and M sites, e(T) and e(M), which overlap within 2σ are also very similar, as well as displacement parameters for T, M and O sites, only TS2E1 showing lower values related to a lower extinction factor.

In the heated crystals, it is worth noting that: (a) The a cell parameter needs the highest T (1150°C) to undergo a small decrease (TS2G3); this is still too small to be attributable to Fe oxidation, as shown by the comparison with a and u collapses in oxidized samples (Table 1, bottom three rows); the a cell parameter does not change significantly in lower-temperature experiments except in TS2D3, in which a small increase is observed. A similar variation also occurred in Larsson's (1995) experiments after heating a natural spinel at low temperature and was attributed to re-adjustment of the spinel crystal. (b) U displacement parameters generally increase with annealing temperature but are lower if the extinction factor is diminished. (c) The number of electrons does not change significantly: e(M), just over 13, suggests – besides Al and Mg residing in the M site – an amount of Fe approximately corresponding to the total estimated Fe^{3+}; e(T), over 15, clearly points to the great amount of Fe in this site. (d) The parameter most sensitive to heat treatment is the oxygen coordinate u, whose variation *vs* temperature is shown in Fig. 1A.

On disordering (upper curve), u undergoes the highest decrease ($\sim$0.0020) at the maximum T reached, 1150°C, (TS2G2-G3), U(Ox) increasing considerably. At 990°C (TS2A4) the u decrease was already significant after 10 min, but further heating at the same temperature caused a further definitive u decrease (TS2A5). At 730°C (TS2C2) the u decrease and U(Ox) increase with respect to the unheated crystals were still significant, while in runs at 650 and 675°C lasting up to one month (TS2D2-D3), the u decrease was very small. Runs at 630 and

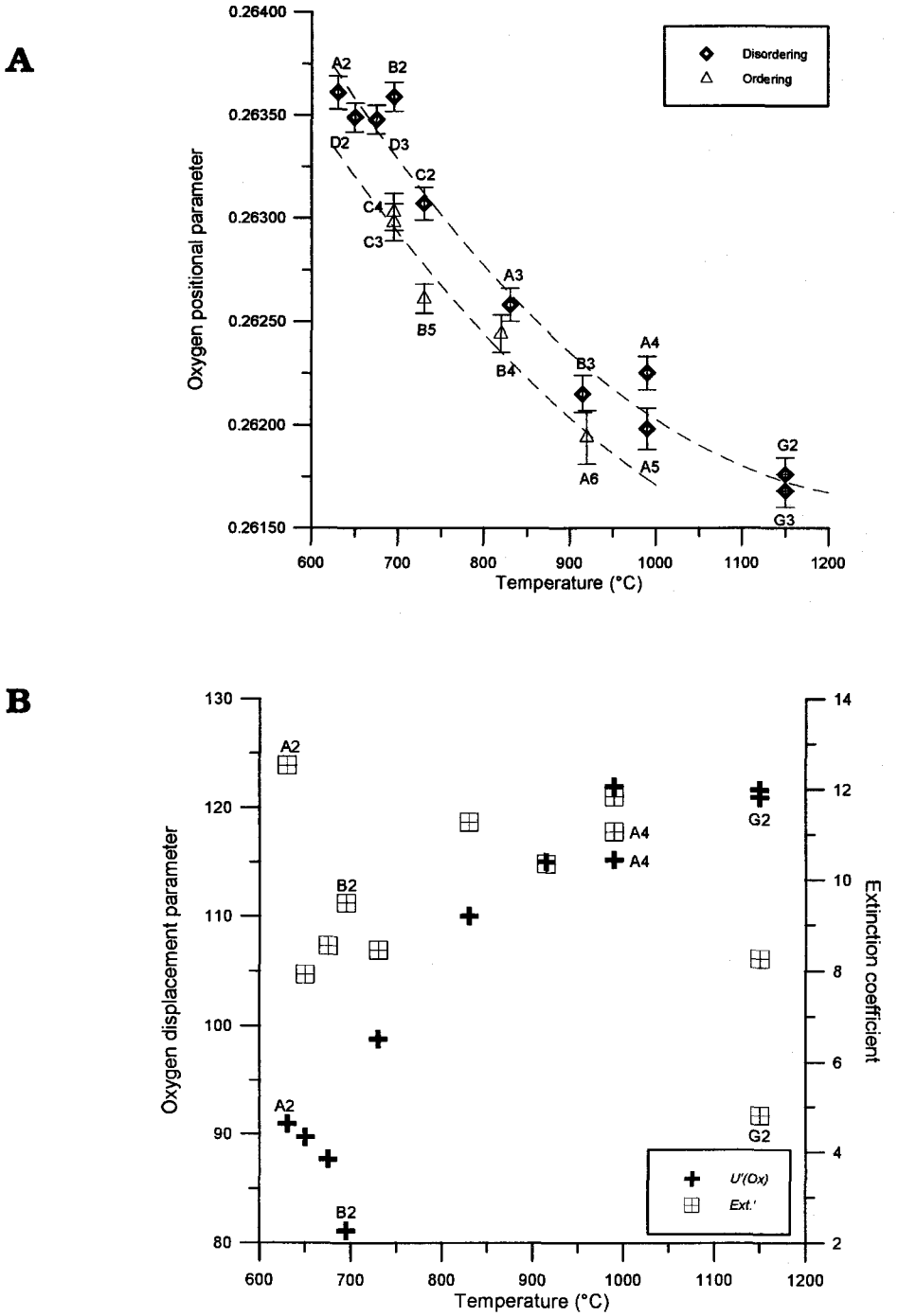

FIG. 1(A) Variations in oxygen coordinate on increasing (disordering) and decreasing (ordering) temperatures in sample TS2. TS2B2 and A4 are off the disordering trend. Data from Table 1. (B) Variations in oxygen displacement parameter and extinction coefficient on increasing temperatures in sample TS2. Note that TS2A2 and G2 are off the *Ext.* trend and TS2B2 is off the $U(\mathrm{Ox})$ trend. $U'(\mathrm{Ox}) = U(\mathrm{Ox})\cdot 10^4$, $Ext.' = Ext\cdot 10^3$. Data from Table 1.

695°C (TS2A2-B2) were performed for a time (~2h) insufficient to give definitive results. Regarding the rate of change *vs* T over 1100°C, crystallographic parameter variations were achieved in a few minutes (TS2G2-G3), while below 1000°C definitely longer times were required (TS2A4-A5).

From the durations of the experiments, it may be concluded that some crystals did not in fact attain equilibrium conditions (TS2A2, B2, A4, G2). This is suggested by the fact that at least one crystallographic parameter – the oxygen coordinate, oxygen displacement parameter or extinction coefficient – was anomalous with respect to the trend of the other crystals (Figs 1A,B).

Results of ordering experiments between 920 and 695°C are also shown in Fig. 1A (lower curve) and marked with an asterisk in Table 1. With decreasing T, only TS2B4 (820°C) reached the u and U(Ox) previously obtained (TS2A3) and TS2A6 (920°C) only reached – within 2σ – the u obtained during disordering at a similar temperature (TS2B3, 915°C), while U displacement parameters remained higher. Run TS2B5 (730°C) did not last long enough to regain the u measured on increasing T (TS2C2), probably like TS2C3-C4 (695°C), whose u values were still significantly lower than in the upper curve.

In conclusion, ordering experiments performed with this technique on spinel crystals show that heating, however realistically prolonged at quite low temperatures, does not last long enough for the crystallographic parameters obtained on disordering to be reached again. In fact, runs at 680°C continued for 120 days (TS2B6, C5, and D4) were unsuccessful precisely because of the difficulties evidenced in the previous section.

Preliminary cation distribution

Cation distribution between the T and M sites in unheated crystals was pursued through a minimization program taking into account both X-ray diffraction data and microprobe analyses.

Assuming a linear dimensional contribution of each cation in a site to the relative bond distance, T–O and M–O may be expressed as $\sum_i X_i R_{\mathrm{T\ or\ M},\,i}$, where X_i and $R_{\mathrm{T\ or\ M},\,i}$ are site cation fractions and bond distances respectively. So substitution of these expressions in equations 1 and 2 gives a and u as functions of X_i, once the oxygen-to-cation distances involved are known.

The values of $R_{\mathrm{T\ or\ M},\,i}$ first used were those of O'Neill and Navrotsky (1983).

The following assumptions were made about cation distribution in our spinels: (a) Mg, Al, $Fe^{2+}$and Fe^{3+} may occupy both T and M sites; (b) minor cations are assigned to only one site, on the basis of their general site preference: Si^{4+} (Urusov, 1983), Mn^{2+} (Rieck and Driessens, 1966; Navrotsky and Kleppa, 1967) and Zn^{2+} (Navrotsky and Kleppa, 1967) to the T site; Cr^{3+} (Navrotsky and Kleppa, 1967; O'Neill and Navrotsky, 1984), Ni^{2+} (Navrotsky and Kleppa, 1967; Urusov, 1983) and Ti^{4+} (Navrotsky and Kleppa, 1967; O'Neill and Navrotsky, 1984) to the M site.

Minimization on each sample was performed by means of the MINUIT program (James and Roos, 1975). The minimized function was:

$$F(X_i) = \sum_{j=1}^{18} \left(\frac{O_j - C_j(X_i)}{\sigma_j} \right)^2 \qquad (3)$$

where O_j is a quantity observed, $C_j(X_i)$ the same quantity calculated by means of parameters X_i, and σ_j the standard deviation of the observed quantity. The 18 quantities were: a, u, e(M), e(T), number of cations both per formula unit and in the T and M sites (3, 1 and 2 respectively), number of charges for the balance, and atomic proportions from microprobe analysis. The X_i parameters chosen were the 14 cation fractions in the two sites.

In the minimization, to point out possible inconsistencies between data obtained from different methods, the cation fractions were allowed to vary without constraints: if the difference between observed and calculated values exceeded 2σ, this would have indicated some inconsistencies in structural and/or chemical data. However, this never occurred in the 23 final minimizations (see below); in fact, the sum of the 18 residuals of equation 3 was ~2 with a maximum of ~5.1, each residual never exceeding 1.6.

In the minimization: (a) all parameters were allowed to vary: cation fractions relative to each species present in both sites were not constrained to have their sum equal to the chemical value; this was also valid for cations present in one site only; (b) for species possibly in both T and M sites, the starting value in each site and the starting step were both set at ½ the cation fraction per formula unit. In this way, the minimum could be searched on a preliminary basis by sweeping the cases from all species in the T site to all species in the M site; (c) for species assigned to only one site, the starting value was set at the chemical value and the starting step at 2 standard deviations. In this way, the minimum could be searched on a preliminary basis among reasonable values of cation fractions; any solution, however, was still allowed; (d) no constraints were imposed on minima and maxima.

Initial results were not acceptable: Fe^{3+} turned out to reside systematically in the T site, while Mössbauer spectroscopic data on the same sample showed strong ordering of Fe^{3+} in the M site and Fe^{2+}

in the T site (Carbonin *et al.*, 1996). This compelled us to revise the set of interatomic distances.

Bond distance optimization and final cation distribution

For a more consistent set of cation bond distances, a database of 83 natural and synthetic samples was prepared, including the TS2 samples refined here and others still unpublished, plus others from the literature, in which a and u (or cation distribution) were both known. They include binary and ternary spinels containing Mg, Al, Fe^{2+}, Fe^{3+}, Cr, Ni and Zn (see Table 3, deposited). All of them should be vacancy-free and not involved in any electron-hopping phenomena. For samples refined with the powder profile technique, the u values were weighted one half, due to lesser accuracy than in single-crystal refinement (Raudsepp *et al.*, 1990; Young, 1995). Data from Peterson *et al.* (1991) for spinel *sensu stricto* were used. Their a value, 8.08435(7) Å, seems to be the only published acceptable value and is consistent both with the data of Tsirel'son *et al.* (1987) and with the value calculated by Lucchesi and Della Giusta (1994) for stoichiometric $MgAl_2O_4$.

Starting cation distributions in samples from literature were taken as published, and in our samples were those obtained as previously described. These data were used to minimize the function:

$$R = \sum_{j=1}^{5} \left(\frac{O_i - C_i}{O_i} \right)^2 \qquad (4)$$

where O_i is a quantity observed and C_i the same quantity calculated from the cation distribution. The five quantities used were: a, T–O and M–O distances, e(T) and e(M).

The variable parameters were twelve bond distances (Mg, Al, Fe^{2+}, Fe^{3+}, Zn, Ni, in the T site; Mg, Al, Fe^{2+}, Fe^{3+}, Cr^{3+}, Ni, in the M site) and an inversion parameter for each sample. For complex compositions, this parameter was changed in subsequent minimization cycles choosing randomly among all possible binary exchanges: Mg-Al, Mg-Fe^{2+}, Mg-Fe^{3+}, Fe^{2+}-Al, Fe^{2+}-Fe^{3+}, Ni-Al. The process was carried out varying ten parameters at a time, randomly chosen among the bond distances and inversion parameters. The procedure was initially stopped far from convergence to avoid forcing towards local minima.

The cation-to-oxygen distances obtained after reaching convergence are reported in Table 4. Bond distances for Si, Mn and Ti were taken from O'Neill and Navrotsky (1983) and not minimized. The estimated accuracy of this set of interatomic distances was ~0.001 Å. In fact, such variations in the bond length of the most abundant species in T and M sites propagate in such a way as to cause a variations of ~0.001 and ~0.002 Å respectively. As these are the typical errors (~2σ) by which a is affected, bond length changes smaller than ~0.001 Å would not cause effectively detectable a changes.

With this set of distances, the cation distribution of each sample of the database was again calculated, as previously described, with equation 3, and satisfactory agreement was found for all of them. In particular, the site populations of the TS2 unheated crystals were in agreement with Mössbauer measurements.

The cation distributions of database samples are reported in Table 3 (deposited), and those of TS2 in Table 5. It should be stressed that, in Table 5, the calculated total number of cations for each species, relative to the same crystal at different T, may occasionally not be constant, due to the absence of constraints when using equation 3 for minimizations. However, the difference between calculated and observed values never exceeded 0.83 σ.

Cation distribution results

In unheated TS2 crystals, iron is highly ordered, Fe^{2+} being mainly in the T site and Fe^{3+} in the M site: $^{[4]}Fe^{3+}$ ranges from 0 to 0.002 afu, $^{[6]}Fe^{2+}$ from 0 to 0.007; these values are probably smaller than the accuracy of the determination. This partitioning is confirmed by Mössbauer spectroscopy. Similar Fe distribution had already been found by Osborne *et al.* (1981) and Chen *et al.* (1992) in chromites, and by

TABLE 4. Radii R_T and R_M (Å) obtained from bond distance optimization and used for cation distribution calculation

	Mg	Fe^{2+}	Fe^{3+}	Al	Mn	Si	Zn	Cr	Ni	Ti
T site	1.965	1.996	1.891	1.767	2.040*	1.652*	1.966		1.974	
M site	2.095	2.138	2.020	1.909				1.996	2.076	1.985*

*From O'Neill and Navrotsky (1983)

Waerenborgh *et al.* (1994) in Zn-Fe-Al spinels from Mössbauer data. The only intracrystalline disorder in our crystals is therefore represented by ~0.12 afu of $^{[4]}$Al and $^{[6]}$Mg.

On increasing T up to 1150°C, a maximum of ~0.12 atoms of $^{[4]}$Mg exchanges with a similar amount of $^{[6]}$Al. Heating does not appear to affect the total iron atoms in each site, as suggested by the very slight variations of e(T) and e(M) (within 2σ) in the same crystal at different T (Table 1). This confirms that increased temperatures did not cause substantial exchanges between light (Mg, Al) and heavy cations (Fe^{2+} or Fe^{3+}). However, in TS2A5 (990°C), TS2G2-G3 (1150°C) and TS2D3 (675°C), Fe^{2+}-Fe^{3+} distribution does appear to be changed slightly, $^{[6]}Fe^{2+}$ reaching ~0.04 and $^{[4]}Fe^{3+}$ ~0.03 afu in TS2G2. The above quantities suggest that the phenomenon at high T was an $^{[4]}Fe^{2+}$-$^{[6]}Fe^{3+}$ exchange, difficult to maintain after quenching. In fact, this disorder was not confirmed after longer heating, particularly for $^{[4]}Fe^{3+}$ (TS2G3).

To sum up, our experiments show that in these spinels, on increasing T, Fe^{2+} exhibits a greater preference than Mg for tetrahedral coordination and only migrates slightly to the M site. The behaviour of Fe^{3+} is not clear, probably due to the very low content of this species (~0.06 afu).

Some previously heated crystals underwent lower T reordering. As already outlined by the u parameter values, some decrease of disorder occurred in terms of Mg-Al distribution, particularly for TS2B4, whose $^{[4]}$Al and $^{[6]}$Mg occupancies were similar to those obtained on disordering TS2A3.

Charge unbalance, oxygen positional and displacement parameters

The proposed cation distribution leads to linear dependence between the oxygen positional parameter and the ratio q(T)/q(M) (charge unbalance), where q(T) and q(M) are the charges in the T and M sites, respectively:

$$u = c_1 \cdot \frac{q(\mathrm{T})}{q(\mathrm{M})} + c_2 \qquad (5)$$

with $c_1 = -0.058$, $c_2 = 0.284$, and $R^2 = 0.994$. This strong correlation (Fig. 2) suggests very close internal consistency both between the data obtained from independent techniques and between the various samples in the series.

The oxygen displacement parameter U(Ox) also depends greatly on both charge unbalance and extinction coefficient. A simple empirical relation between the former quantities is:

$$U(\mathrm{Ox}) = c_1 \cdot \frac{q(\mathrm{T})}{q(\mathrm{M})} + c_2 \cdot \left(\frac{q(\mathrm{T})}{q(\mathrm{M})}\right)^2 + c_3 \cdot \frac{1}{Ext.} + c_4 \qquad (6)$$

The best coefficients found from our data were: $c_1 = -0.1537$, $c_2 = 0.3562$, $c_3 = -9{\cdot}10^{-6}$, $c_4 = 0.0187$, and $R^2 = 0.962$. Equation 6 reproduces the great majority of displacement parameters within 1σ and all of them within 4σ.

When thermal runs are performed, equations 5 and 6 are useful in checking parameter reliability and the consistency of cation distributions.

Temperature-dependent Al distribution

According to our experimental data, Al partitioning between the T and M sites is primarily controlled by the annealing temperature. Some scattering may be due to the presence of other cations, different from Mg and Al, in the T and M sites. Correcting for the effect of foreign ions, a thermometric experimental function is obtained in the form:

$$T = c_1 + c_2 B + c_3 B^2 \ (^\circ\mathrm{C}) \qquad (7)$$

where

$$B = {}^{[4]}\mathrm{Al}/({}^{[4]}\mathrm{Al} + {}^{[6]}\mathrm{Al}) + c_4(1 - {}^{[4]}\mathrm{Mg} - {}^{[4]}\mathrm{Al}) + c_5(2 - {}^{[6]}\mathrm{Mg} - {}^{[6]}\mathrm{Al}) \qquad (8)$$

and $c_1 = 1252.9$, $c_2 = -13953$, $c_3 = 83524$, $c_4 = 0.08419$, $c_5 = 0.040035$.

The coefficients of equation 7 were obtained by fitting the temperatures of runs in which equilibrium was attained (TS2A3, A5, B3, C2, D2, D3 and G3) and data from one unpublished run on a chromite sample (CR5A2), reported in Table 3 (deposited). The latter was included for a better estimate of the third term of equation 8, since its cation distribution was very different from TS2 spinels in terms of $^{[6]}$Mg and $^{[6]}$Al contents.

Equation 7 is experimental: in general it should hold for spinels up to 1150°C in which temperature does not cause appreciable disorder in cations different from Al and Mg. The temperatures of the eight experimental data used are reproduced with 13°C as mean difference and 27°C as maximum. For the unheated TS2 crystals, a temperature of ~670°C was calculated, which may represent the threshold for intracrystalline exchanges; this temperature agrees with the results of Yamanaka and Takeuchi (1983) in synthetic $MgAl_2O_4$. For comparison with other experimental results, annealing temperatures were calculated on four quenched samples of $MgAl_2O_4$ by Millard *et al.* (1992), with 35°C as mean difference and 88°C as maximum, relative to one sample approaching equilibrium distribution from a previously lower equilibration temperature.

TABLE 5. Cation distributions in TS2 and comparison between observed and calculated structural parameters: obs. from structure refinement, calc. from cation distribution

Sample	site	Al	Fe^{2+}	Fe^{3+}	Mg	Mn	Si	Zn	Cr	Ni	Ti		*a*	*u*	*e*(T)	*e*(M)
TS2A 1	T	0.1224	0.2203	0.0000	0.6526	0.0024		0.0020				obs.	8.1104	0.26362	15.26	13.38
	M	1.8130	0.0033	0.0581	0.1181				0.0065		0.0007	calc.	8.1105	0.26361	15.27	13.37
2	T	0.1234	0.2215	0.0000	0.6504	0.0024		0.0020				obs.	8.1099	0.26361	15.38	13.43
	M	1.8119	0.0027	0.0586	0.1193				0.0065		0.0007	calc.	8.1100	0.26360	15.29	13.37
3	T	0.1986	0.2231	0.0000	0.5738	0.0024		0.0020				obs.	8.1106	0.26258	15.48	13.38
	M	1.7364	0.0031	0.0574	0.1960				0.0065		0.0007	calc.	8.1106	0.26258	15.39	13.33
4	T	0.2231	0.2255	0.0000	0.5469	0.0025		0.0020				obs.	8.1100	0.26225	15.63	13.39
	M	1.7117	0.0015	0.0576	0.2220				0.0065		0.0007	calc.	8.1100	0.26225	15.45	13.31
5	T	0.2411	0.2173	0.0006	0.5365	0.0025		0.0020				obs.	8.1100	0.26198	15.60	13.46
	M	1.6937	0.0098	0.0568	0.2325				0.0065		0.0007	calc.	8.1100	0.26198	15.36	13.36
6*	T	0.2442	0.2150	0.0000	0.5363	0.0024		0.0020				obs.	8.1096	0.26194	15.34	13.37
	M	1.6909	0.0101	0.0572	0.2346				0.0065		0.0007	calc.	8.1096	0.26194	15.32	13.36
TS2B 1	T	0.1222	0.2169	0.0000	0.6552	0.0021	0.0011	0.0025				obs.	8.1108	0.26361	15.28	13.40
	M	1.8147	0.0006	0.0477	0.1170				0.0127	0.0068	0.0005	calc.	8.1108	0.26361	15.23	13.38
2	T	0.1201	0.2167	0.0089	0.6486	0.0021	0.0011	0.0024				obs.	8.1113	0.26359	15.38	13.33
	M	1.8158	0.0000	0.0394	0.1248				0.0127	0.0068	0.0005	calc.	8.1113	0.26359	15.35	13.32
3	T	0.2280	0.2156	0.0000	0.5506	0.0021	0.0011	0.0025				obs.	8.1089	0.26215	15.40	13.41
	M	1.7061	0.0051	0.0504	0.2183				0.0127	0.0068	0.0005	calc.	8.1089	0.26215	15.32	13.37
4*	T	0.2064	0.2220	0.0040	0.5619	0.0021	0.0011	0.0026				obs.	8.1094	0.26244	15.55	13.36
	M	1.7277	0.0000	0.0465	0.2057				0.0127	0.0068	0.0005	calc.	8.1094	0.26244	15.44	13.32
5*	T	0.1927	0.2192	0.0065	0.5759	0.0021	0.0011	0.0025				obs.	8.1097	0.26261	15.47	13.33
	M	1.7423	0.0000	0.0430	0.1947				0.0127	0.0068	0.0005	calc.	8.1097	0.26261	15.43	13.30
TS2C 1	T	0.1270	0.2187	0.0004	0.6481	0.0021	0.0011	0.0025				obs.	8.1113	0.26354	15.33	13.41
	M	1.8079	0.0000	0.0490	0.1231				0.0127	0.0068	0.0005	calc.	8.1113	0.26354	15.27	13.38
2	T	0.1597	0.2251	0.0062	0.6032	0.0022	0.0010	0.0026				obs.	8.1105	0.26307	15.60	13.39
	M	1.7736	0.0000	0.0454	0.1608				0.0127	0.0069	0.0005	calc.	8.1105	0.26307	15.47	13.34
3*	T	0.1686	0.2225	0.0000	0.6030	0.0021	0.0010	0.0026				obs.	8.1097	0.26298	15.55	13.46
	M	1.7661	0.0017	0.0505	0.1616				0.0127	0.0069	0.0005	calc.	8.1098	0.26297	15.36	13.38
4*	T	0.1627	0.2219	0.0042	0.6055	0.0022	0.0011	0.0025				obs.	8.1111	0.26303	15.50	13.39
	M	1.7694	0.0000	0.0482	0.1625				0.0127	0.0068	0.0005	calc.	8.1111	0.26303	15.40	13.35

TABLE 5. (*contd.*)

Sample	site	Al	Fe^{2+}	Fe^{3+}	Mg	Mn	Si	Zn	Cr	Ni	Ti		*a*	*u*	*e*(T)	*e*(M)
TS2D 1	T	0.1224	0.2313	0.0000	0.6422	0.0020		0.0021				obs.	8.1143	0.26361	15.44	13.51
	M	1.8013	0.0068	0.0554	0.1105				0.0190	0.0060	0.0010	calc.	8.1143	0.26361	15.42	13.50
2	T	0.1319	0.2383	0.0012	0.6245	0.0020		0.0022				obs.	8.1138	0.26349	15.60	13.47
	M	1.7913	0.0000	0.0552	0.1274				0.0190	0.0062	0.0008	calc.	8.1138	0.26349	15.55	13.45
3	T	0.1146	0.2076	0.0336	0.6399	0.0021		0.0022				obs.	8.1151	0.26348	15.61	13.47
	M	1.8081	0.0308	0.0231	0.1120				0.0190	0.0062	0.0008	calc.	8.1151	0.26348	15.56	13.45
TS2E 1	T	0.1211	0.2205	0.0019	0.6533	0.0019	0.0008	0.0001				obs.	8.1081	0.26363	15.31	13.35
	M	1.8208	0.0000	0.0522	0.1178				0.0031	0.0052	0.0005	calc.	8.1084	0.26363	15.26	13.34
TS2F 1	T	0.1232	0.2233	0.0000	0.6487	0.0021	0.0007	0.0019				obs.	8.1122	0.26359	15.27	13.43
	M	1.8068	0.0023	0.0576	0.1147				0.0099	0.0079	0.0008	calc.	8.1122	0.26359	15.31	13.45
TS2G 1	T	0.1191	0.2370	0.0011	0.6394	0.0018		0.0016				obs.	8.1136	0.26367	15.40	13.38
	M	1.8078	0.0000	0.0494	0.1157				0.0181	0.0067	0.0024	calc.	8.1136	0.26367	15.50	13.42
2	T	0.2421	0.2024	0.0264	0.5248	0.0021		0.0022				obs.	8.1121	0.26176	15.56	13.50
	M	1.6806	0.0360	0.0293	0.2272				0.0180	0.0072	0.0018	calc.	8.1121	0.26176	15.51	13.47
3	T	0.2628	0.2267	0.0000	0.5067	0.0019		0.0019				obs.	8.1107	0.26168	15.48	13.45
	M	1.6618	0.0111	0.0535	0.2466				0.0180	0.0070	0.0020	calc.	8.1107	0.26168	15.50	13.46

* Ordering runs.

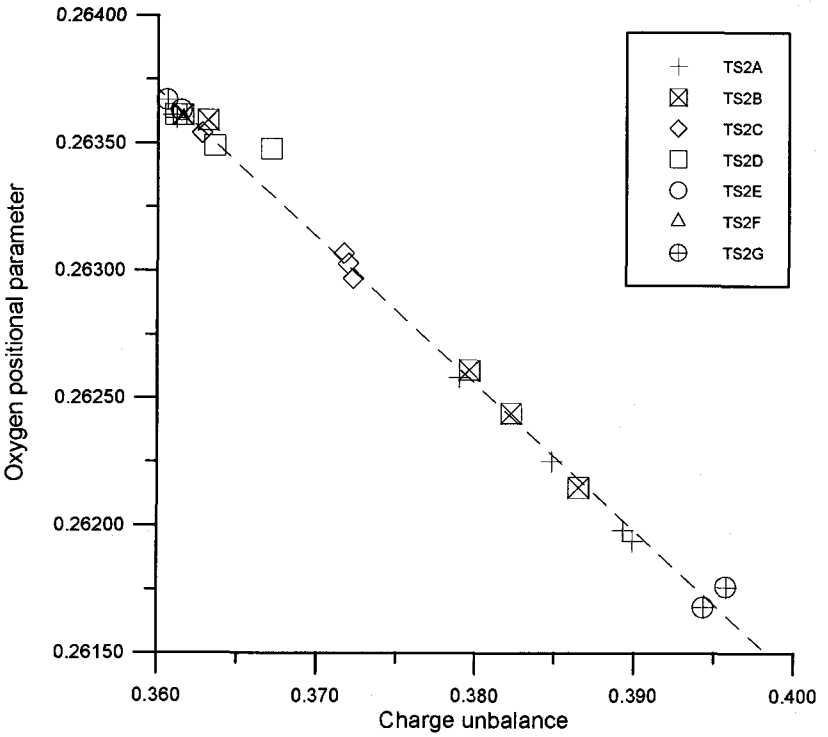

FIG. 2. Oxygen coordinate parameter u *vs* $q(T)/q(M)$ plot in unheated and heated TS2 crystals. Values calculated from cation distributions (Table 5).

Conclusions

The TS2 natural spinel shows strong enrichment of Mg and Fe^{2+} in tetrahedral site, while the M site is mainly filled by Al and (to a lesser extent) by Fe^{3+}.

There is no clear evidence of substantial changes in Fe^{2+}-Fe^{3+} distribution after heating and quenching. Instead, ~0.12 afu of Mg and Al exchange between the two sites at 1150°C.

Quenching at 1150°C seems to have been effective, to judge from the oxygen coordinate value, which is decreased with respect to that of 990°C.

Ordering experiments performed on single spinel crystals were successful only at higher temperatures. Prolonged heating, necessary at lower temperatures, involves considerable drawbacks from a technical viewpoint.

Cation distributions *vs T* are different from those proposed by Nell *et al.* (1989) in synthetic spinels, "quite rich in magnetite". In TS2, "the small amount of magnetite end-member was probably responsible for the different behaviour of Fe^{3+}" with respect to the synthetic solid solution. The ordering scheme in our samples, in fact, is completely different from that of magnetite, since all Fe^{2+}, even before heating, is virtually in the T site and all Fe^{3+} in the M site thus preventing the possibility of electron hopping. The results of Nell *et al.* (1989) therefore cannot be compared with ours.

Reappraisal and improvement of bond distances in spinel structure are necessary to fit measured and calculated cation distributions of Fe^{2+} and Fe^{3+}. The Mg-Al exchange *vs T* allowed the formulation of a thermometric relation, which was tested with a satisfactory fit on an $MgAl_2O_4$ synthetic spinel, similar to ours in composition.

The oxidation observed in some samples during heating will be the subject of further investigation, as well as short-range ordering – highlighted by Mössbauer spectroscopy – which may play a role in *T* reversal experiments.

Acknowledgements

Comments by H.St.C. O'Neill and by an anonymous referee substantially improved this manuscript. This work was supported by MURST project 'Cristallochimica e Termodinamica dei minerali'.

References

Basso, R., Comin-Chiaramonti, P., Della Giusta, A. and Flora, O. (1984) Crystal chemistry of four Mg-Fe-Al-Cr spinels from the Balmuccia peridotite (Western Italian Alps). *Neues Jahrb. Mineral. Abh.*, **150**, 1–10.

Blessing, R.H., Coppens, P. and Becker, P. (1972) Computer analysis of step-scanned X-ray data. *J. Appl. Cryst.*, **7**, 488–92.

Carbonin, S., Russo, U. and Della Giusta, A. (1996) Cation distribution in some natural spinels from X-ray diffraction and Mössbauer spectroscopy. *Mineral. Mag.*, **60**, 355–68.

Chen, Y.L., Xu, B.F., Chen, J.G. and Ge, Y.Y. (1992) Fe^{2+}-Fe^{3+} ordered distribution in chromite spinels. *Phys. Chem. Miner.*, **19**, 255–9.

Comin-Chiaramonti, P., Demarchi, G., Siena, F. and Sinigoi, S. (1982) Relazioni tra fusione e deformazione nella peridotite di Balmuccia (Ivrea-Verbano). *Rend. Soc. Ital. Mineral. Petrol.*, **38**, 685–700.

Cynn, H., Anderson, O.L. and Nicol, H. (1993) Effects of cation ordering in a natural $MgAl_2O_4$ spinel observed by rectangular parallelepiped ultrasonic resonance and Raman measurements. *Pure Appl. Geophys.*, **141**, 415–44.

Della Giusta, A. and Ottonello, G. (1993) Energy and long-range disorder in simple spinels. *Phys. Chem. Miner.*, **20**, 228–41.

Della Giusta, A., Princivalle, F. and Carbonin, S. (1986) Crystal chemistry of a suite of natural Cr-bearing spinels with $0.15 < Cr < 1.07$. *Neues Jahrb. Mineral. Abh.*, **155**, 319–30.

Della Giusta, A., Princivalle, F. and Carbonin, S. (1987) Crystal structure and cation distribution in some natural magnetites. *Mineral. Petrol.*, **37**, 315–21.

Gasparik, T. and Newton, R.C. (1984) The reversed alumina contents of orthopyroxene in equilibrium with spinel and forsterite in the system MgO-Al_2O_3-SiO_2. *Contrib. Mineral. Petrol.*, **85**, 186–96.

Grimes, N.W., Thompson, P. and Kay, H.F. (1982) New symmetry and structure for spinel. *Proc. Royal Soc. London*, **A386**, 333–45.

Hafner, S. (1960) Metalloxyde mit Spinellstruktur. *Schw. Miner. Petr. Mitt.*, **40**, 208–40.

Hill, R.J., Craig, J.R. and Gibbs, G.V. (1979) Systematics of the spinel structure type. *Phys. Chem. Mineral.*, **4**, 317–39.

Irvine, T.N. (1965) Chromian spinel as a petrogenetic indicator. Part 1. Theory. *Canad. J. Earth Sci.*, **2**, 648–72.

James, F. and Roos, M. (1975) MINUIT, A system for function minimization and analysis of the parameters errors and correlations. *Comp. Phys. Comm.*, **10**, 343–67.

Larsson, L. (1995) Temperature dependent cation distribution in a natural $Mg_{0.4}Fe_{0.6}Al_2O_4$ spinel. *Neues Jahrb. Mineral. Mh.*, 173–84.

Larsson, L., O'Neill, H.St.C. and Annersten, H. (1994) Crystal chemistry of synthetic hercynite ($FeAl_2O_4$) from XRD structural refinements and Mössbauer spectroscopy. *Eur. J. Mineral.*, **6**, 39–51.

Lucchesi, S. and Della Giusta, A. (1994) Crystal chemistry of non-stoichiometric Mg-Al synthetic spinels. *Zeit. Kristallogr.*, **209**, 714–9.

Millard, R.L., Peterson, R.C. and Hunter, B.K. (1992) Temperature dependence of cation disorder in $MgAl_2O_4$ spinel using ^{27}Al and ^{17}O magic-angle spinning NMR. *Amer. Mineral.*, **77**, 44–52.

Navrotsky, A. and Kleppa, O.J. (1967) The thermodynamics of cation distribution in simple spinels. *J. Inorg. Nucl. Chemistry*, **29**, 2701–14.

Nell, J., Wood, B.J. and Mason, T.O. (1989) High temperature cation distributions in Fe_3O_4 - $MgAl_2O_4$ - $MgFe_2O_4$ - $FeAl_2O_4$ spinels from thermopower and conductivity measurements. *Amer. Mineral.*, **74**, 339–51.

North, A.C.T., Phillips, D.C. and Scott-Mattews, F. (1968) A semi-empirical method of absorption correction. *Acta Cryst.*, **A24**, 351–2.

O'Neill, H.St.C. (1992) Temperature dependence of the cation distribution in zinc ferrite ($ZnFe_2O_4$) from powder XRD structural refinements. *Eur. J. Mineral.*, **4**, 571–80.

O'Neill, H.St.C. and Dollase, W.A. (1993) Crystal structures and cation distributions in simple spinels from powder XRD structural refinements: $MgCr_2O_4$, $ZnCr_2O_4$, Fe_3O_4 and the temperature dependence of the cation distribution in $ZnAl_2O_4$. *Phys. Chem. Miner.*, **20**, 541–55.

O'Neill, H.St.C. and Navrotsky, A. (1983) Simple spinels: crystallographic parameters, cation radii, lattice energies, and cation distribution. *Amer. Mineral.*, **68**, 181–94.

O'Neill, H.St.C. and Navrotsky, A. (1984) Cation distribution and thermodynamic properties of binary spinel solid solutions. *Amer. Mineral.*, **69**, 733–53.

O'Neill, H.St.C., Dollase W.A. and Ross, C.R.II (1991) Temperature dependence of the cation distribution in Nickel Aluminate ($NiAl_2O_4$) spinel: a powder XRD study. *Phys. Chem. Miner.*, **18**, 302–19.

O'Neill, H.St.C., Annersten, H. and Virgo, D. (1992) The temperature dependence of the cation distribution in magnesioferrite ($MgFe_2O_4$) from powder XRD structural refinements and Mössbauer spectroscopy. *Amer. Mineral.*, **77**, 725–40.

Osborne, M.D., Fleet, M.E. and Bancroft, G.M. (1981)

Fe^{2+}-Fe^{3+} ordering in chromite and Cr-bearing spinels. *Contrib. Mineral. Petrol.*, **77**, 251–5.

Ottonello, G. (1986) Energetics of multiple oxides with spinel structure. *Phys. Chem. Miner.*, **13**, 79–90.

Peterson, R.C., Lager, G.A. and Hitterman, R.L. (1991) A time-of-flight neutron powder diffraction study of $MgAl_2O_4$ at temperatures up to 1273 K. *Amer. Mineral.*, **76**, 1455–8.

Petric, A. and Jacob, K.T. (1982) Thermodynamic properties of Fe_3O_4 - FeV_2O_4 and Fe_3O_4 - $FeCr_2O_4$ spinel solid solutions. *J. Amer. Ceramic Soc.*, **65**, 117–23.

Pizzolon, M. (1991) *Cristallochimica e modellizzazione di spinelli di Mg-Al-Fe-Cr.* Thesis, University of Padova, Padova, Italy.

Princivalle, F., Della Giusta, A. and Carbonin, S. (1989) Comparative crystal chemistry of spinels from some suites of ultramafic rocks. *Mineral. Petrol.*, **40**, 117–26.

Raudsepp, M., Hawthorne, F.C. and Turnock, A.C. (1990) Evaluation of the Rietveld method for the characterization of fine-grained products of mineral synthesis: the diopside-hedenbergite join. *Canad. Mineral.*, **28**, 93–109.

Rieck, G.D. and Driessens, F.C.M. (1966) The structure of manganese-iron-oxygen spinels. *Acta Cryst.*, **20**, 521–5.

Sack, R.O. (1982) Spinels as petrogenetic indicators: activity-composition relations at low pressure. *Contrib. Mineral. Petrol.*, **79**, 169–86.

Sack, R.O. and Ghiorso, M.S. (1991*a*) Chromian spinels as petrogenetic indicators: thermodynamics and petrological applications. *Amer. Mineral.*, **76**, 827–47.

Sack, R.O. and Ghiorso, M.S. (1991*b*) An internally consistent model for the thermodynamic properties of Fe-Mg-titanomagnetite-aluminate spinels. *Contrib. Mineral. Petrol.*, **106**, 474–505.

Sheldrick, G.M. (1993) *SHELX-93. Program for crystal structure refinement.* University of Göttingen, Germany.

Schmocker, U. and Waldner, F. (1976) The inversion parameter with respect to space group of $MgAl_2O_4$ spinels. *J. Phys., C: Solid State Physics*, **9**, L235–7.

Trestman-Matts, A., Dorris, S.E., Kumarakrishnan, S. and Mason, T.O. (1983) Thermoelectric determination of cation distributions in Fe_3O_4-Fe_2TiO_4. *J. Amer. Ceramic Soc.*, **66**, 829–34.

Tsirel'son, V.G., Belokoneva, Ye. L., Nozik, Yu. Z. and Urusov, V.S. (1987) Precision X-ray diffraction data on the structure of $MgAl_2O_4$ spinel. *Geochem. Intern.*, **24(2)**, 124–30.

Urusov, V.S. (1983) Interaction of cations on octahedral and tetrahedral sites in simple spinels. *Phys. Chem. Mineral.*, **9**, 1–5.

Waerenborgh, J.C., Figueiredo, M.O., Cabral, J.M.P. and Pereira, I.C.J. (1994) Powder XRD structure refinements and ^{57}Fe Mössbauer effect study of synthetic $Zn_{1-x}Fe_xAl_2O_4$ ($0 < x \leqslant 1$) spinels annealed at different temperatures. *Phys. Chem. Miner.*, **21**, 460–8.

Wu, C.C. and Mason, T.O. (1981) Thermopower measurement of cation distribution in magnetite. *J. Amer. Ceramic Soc.*, **64**, 520–2.

Yamanaka, T. and Takeuchi, Y. (1983) Order-disorder transition in $MgAl_2O_4$ spinel at high temperatures up to 1700°C. *Zeit. Kristall.*, **165**, 65–78.

Young, R.A. (1995) Introduction to the Rietveld method. In *The Rietveld Method* (R.A. Young, ed.). International Union of Crystallography, Oxford University Press Inc., New York, pp. 1–38.

[*Manuscript received 13 April 1995: revised 7 November 1995*]